

Supporting Information for:

## Preparation of Monodisperse Cerium Oxide Particle Suspensions from a Tetravalent Precursor

Ashley M. Hastings,<sup>1</sup> Susana Herrera,<sup>2</sup> Sharee Harris,<sup>3</sup> Tashi Parsons-Davis,<sup>1</sup> Andrew J. Pascall,<sup>4</sup> and Jennifer A. Shusterman<sup>1\*</sup>

<sup>1</sup>*Nuclear and Chemical Sciences Division, Lawrence Livermore National Laboratory, Livermore, CA 94550, USA*

<sup>2</sup>*Florida International University, Miami, FL 33199, USA. Pacific Northwest National Laboratory, Richland, WA 99352, USA*

<sup>3</sup>*Materials Science Division, Lawrence Livermore National Laboratory, Livermore, CA 94550, USA*

<sup>4</sup>*Materials Engineering Division, Lawrence Livermore National Laboratory, Livermore, CA 94550, USA*

\*corresponding author | email: [shusterman1@llnl.gov](mailto:shusterman1@llnl.gov)

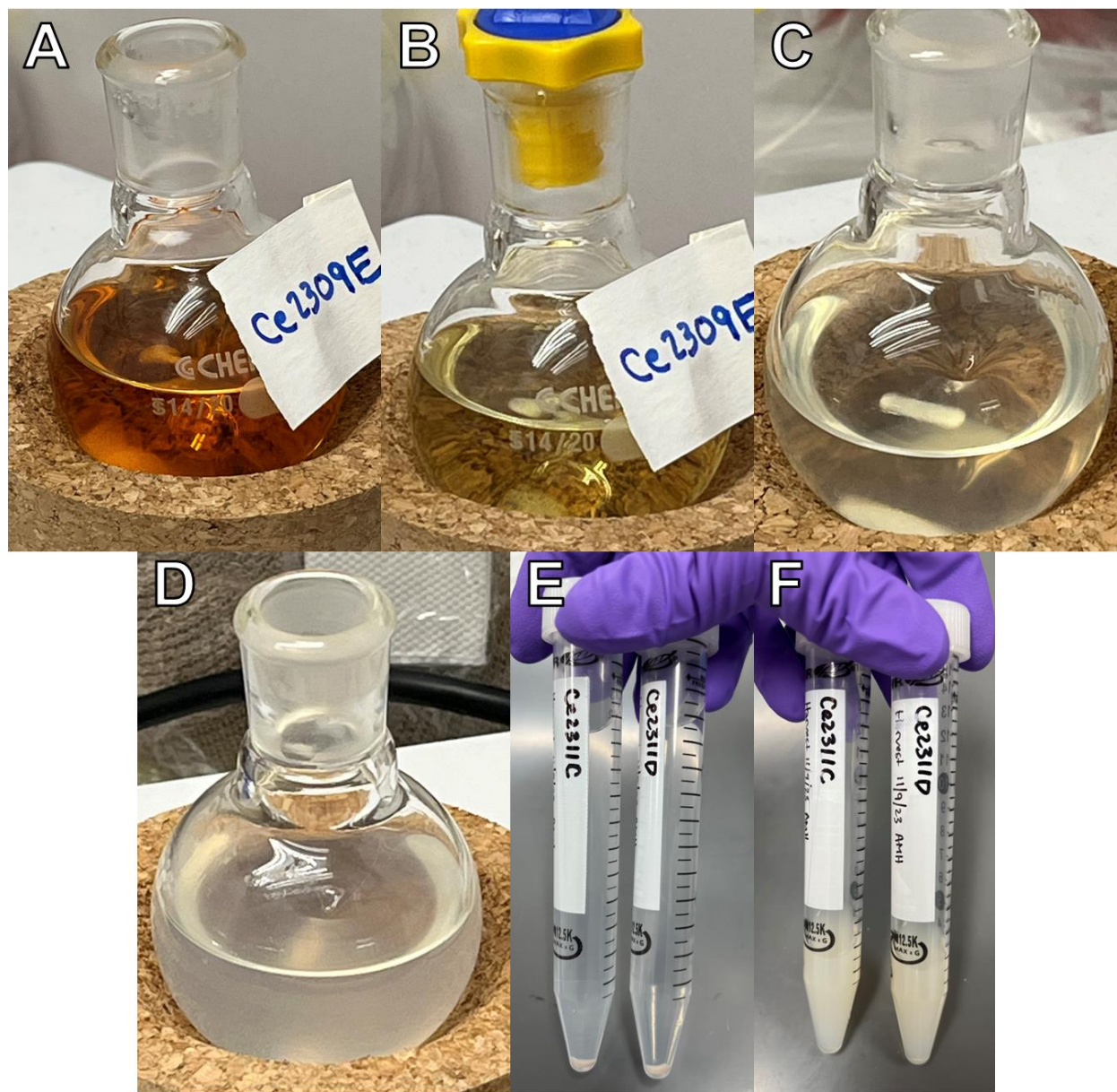


Figure S1. Photos from the Ce particle synthesis. A) Cerium solution added to a mixture of water, ethanol, and HMT. B) After 15 minutes of stirring. C) After pH adjusting from  $\sim 1.1$  to 1.4. D) Cloudiness indicating initial particle formation ( $1.5 < \text{pH} < 7.5$ ). E) Particle pellets centrifuged with ethanol wash. F) Washed Ce particles in ethanol suspension.

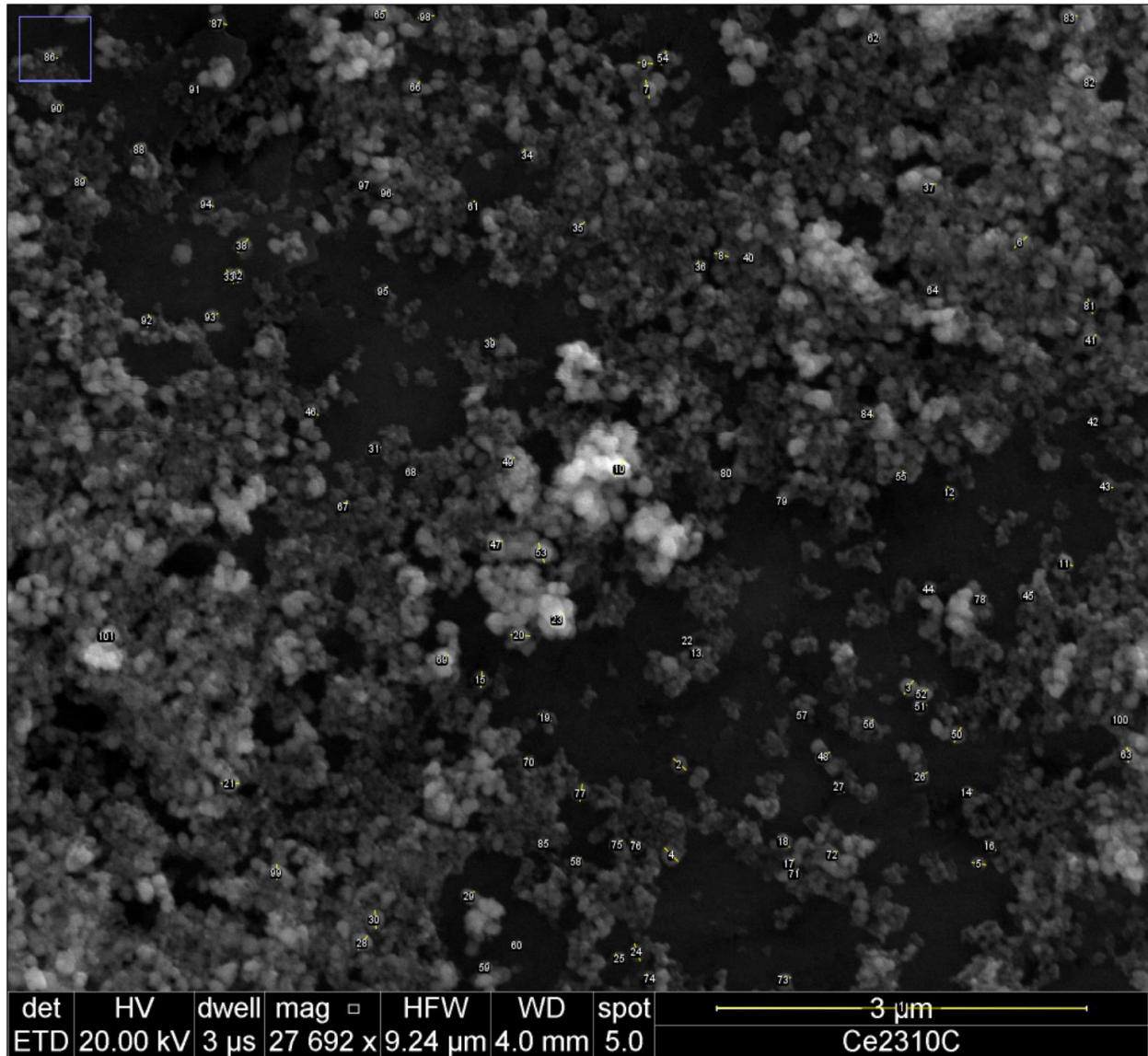


Figure S2. Scanning electron micrograph of cerium particles synthesized at pH 1.9. The 100 particles sampled for particle size through ImageJ are shown.



Figure S3. Magnified inset of micrograph from Figure S2 to highlight a sampling of particle diameter line selections in ImageJ software.

Table S1. Compilation of the particle diameter measurements from Image J. Line #1 (not included) indicates the 3  $\mu\text{m}$  scale bar from the scanning electron micrograph.

Particle	Diameter (nm)	Particle	Diameter (nm)	Particle	Diameter (nm)	Particle	Diameter (nm)	Particle	Diameter (nm)
2	134	22	69	42	90	62	81	82	92
3	129	23	137	43	96	63	113	83	120
4	153	24	141	44	99	64	87	84	103
5	111	25	99	45	98	65	112	85	88
6	131	26	119	46	111	66	105	86	109
7	142	27	105	47	115	67	101	87	139
8	113	28	132	48	118	68	77	88	88
9	118	29	100	49	113	69	109	89	96
10	143	30	149	50	129	70	93	90	94
11	118	31	94	51	94	71	94	91	80
12	109	32	99	52	106	72	94	92	100
13	107	33	115	53	161	73	113	93	111
14	103	34	114	54	117	74	95	94	108
15	131	35	121	55	91	75	109	95	106
16	106	36	103	56	100	76	99	96	104
17	99	37	99	57	45	77	141	97	96
18	118	38	129	58	96	78	99	98	124
19	115	39	95	59	90	79	85	99	122
20	154	40	68	60	65	80	74	100	85
21	149	41	110	61	88	81	117	101	112
<b>Average <math>\pm 2\sigma</math></b>								<b>108 <math>\pm 41</math></b>	

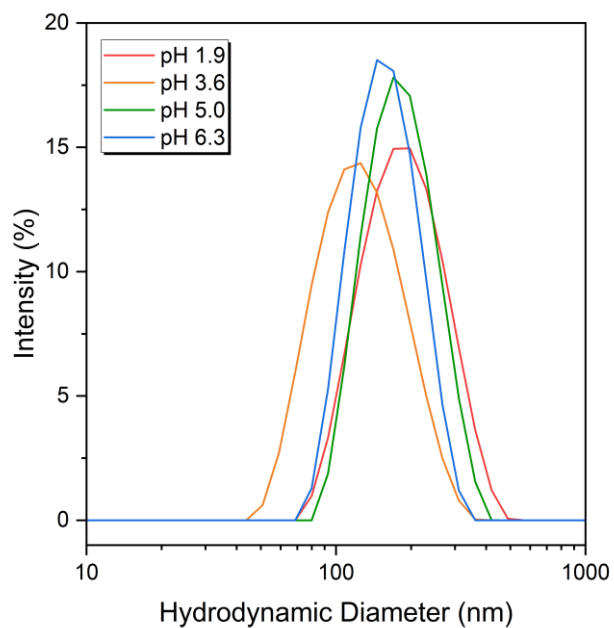


Figure S4. Dynamic light scattering intensity distributions of Ce particle batches synthesized at the indicated pHs. Data were collected on the day the particles were harvested.

Table S2.  $Z_{avg}$ , polydispersity index (PDI), and zeta potential values corresponding to the samples displayed in Figure 1 and Figure S4.

<b>Synthesis pH</b>	<b><math>Z_{avg} \pm 2\sigma</math> (nm)</b>	<b><math>PDI \pm 2\sigma</math></b>	<b>Zeta Potential (mV)</b>
<b>1.9</b>	$175 \pm 2$	$0.103 \pm 0.033$	+28.8
<b>3.6</b>	$115 \pm 1$	$0.112 \pm 0.023$	+40.0
<b>5.0</b>	$172 \pm 2$	$0.0988 \pm 0.0363$	+35.5
<b>6.3</b>	$149 \pm 3$	$0.0807 \pm 0.0596$	+55.0

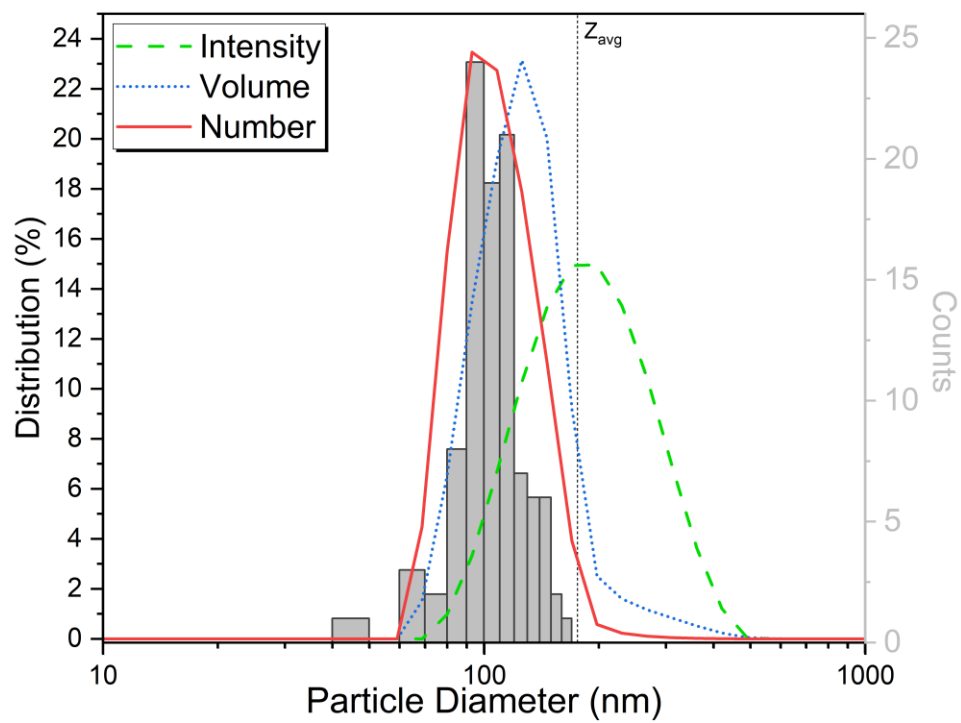


Figure S5. Comparison of the hydrodynamic diameter volume distribution to the particle size distribution determined via scanning electron microscopy.

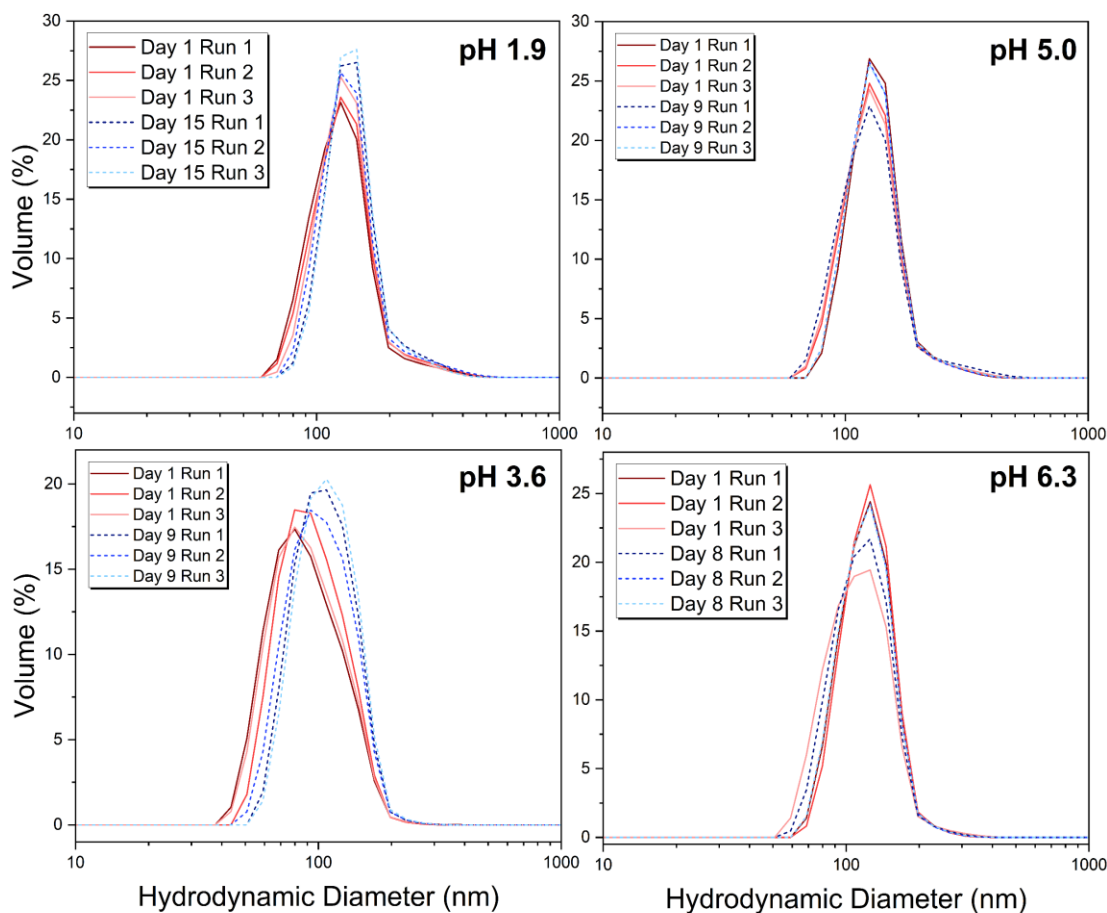


Figure S6. Dynamic light scattering volume distributions of Ce particle batches at the indicated pHs with the initial vs. aged characterization.

Table S3. Comparison of initial and aged  $Z_{\text{avg}}$  values for the Ce particle samples plotted in Figure S6.

Synthesis pH	Day 1 $Z_{\text{avg}} \pm 2\sigma$ (nm)	Aged $Z_{\text{avg}} \pm 2\sigma$ (nm)
<b>1.9</b>	$175 \pm 2$	$184 \pm 4$
<b>3.6</b>	$115 \pm 1$	$128 \pm 4$
<b>5.0</b>	$172 \pm 2$	$174 \pm 10$
<b>6.3</b>	$149 \pm 3$	$148 \pm 1$

Table S4. Comparison of initial and aged polydispersity indexes for the Ce particle samples plotted in Figure S6.

Synthesis pH	Day 1 PDI $\pm 2\sigma$	Aged PDI $\pm 2\sigma$
<b>1.9</b>	$0.103 \pm 0.033$	$0.0792 \pm 0.0517$
<b>3.6</b>	$0.112 \pm 0.023$	$0.0765 \pm 0.0133$
<b>5.0</b>	$0.0988 \pm 0.0363$	$0.0993 \pm 0.0185$
<b>6.3</b>	$0.0807 \pm 0.0596$	$0.0712 \pm 0.0169$



Figure S7. Comparison of relatively dilute (left) and relatively concentrated (right) Ce particle suspensions.

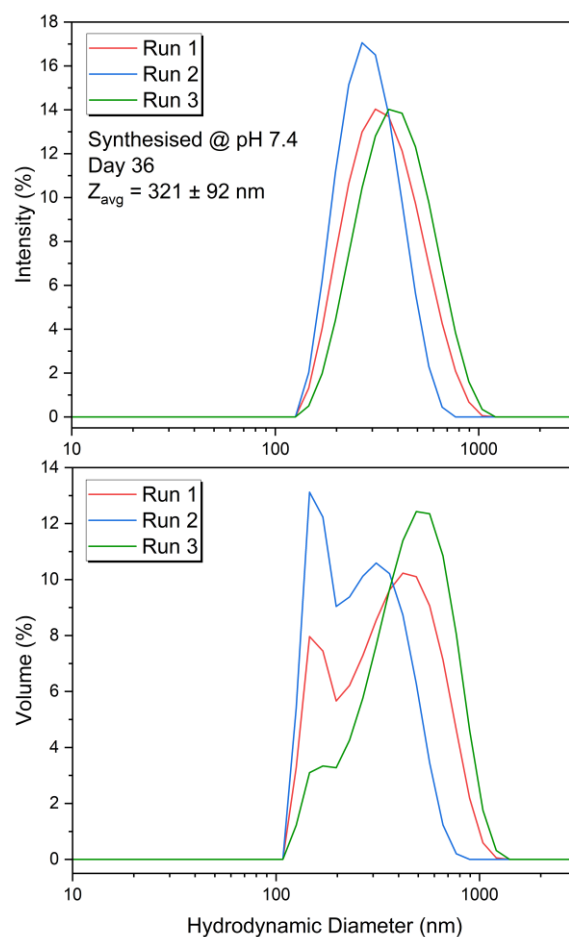


Figure S8. Intensity (top) and volume (bottom) distributions of the same Ce particle batch that reveals multiple particle populations due to incomplete dispersion via ultrasonication during sample preparation.



Table S5. Quantities of the additives explored with the Ce particle suspensions. The indicated amounts were added to 100  $\mu\text{L}$  of the Ce particle batch in ethanol.

Additive	Volume ( $\mu\text{L}$ )	Comment
Acetylacetone (acac)	5	5% v
Darvan 821A	$\sim 1$	1% v, viscous
Polyethyleneimine (PEI, 800 MW, branched)	$\sim 1$	1% v, viscous
H <sub>2</sub> O	12.5	Control for aqueous additives
Urea (4 M)	12.5	Molar eq. to acac
Citric acid (4 M)	12.5	Molar eq. to acac

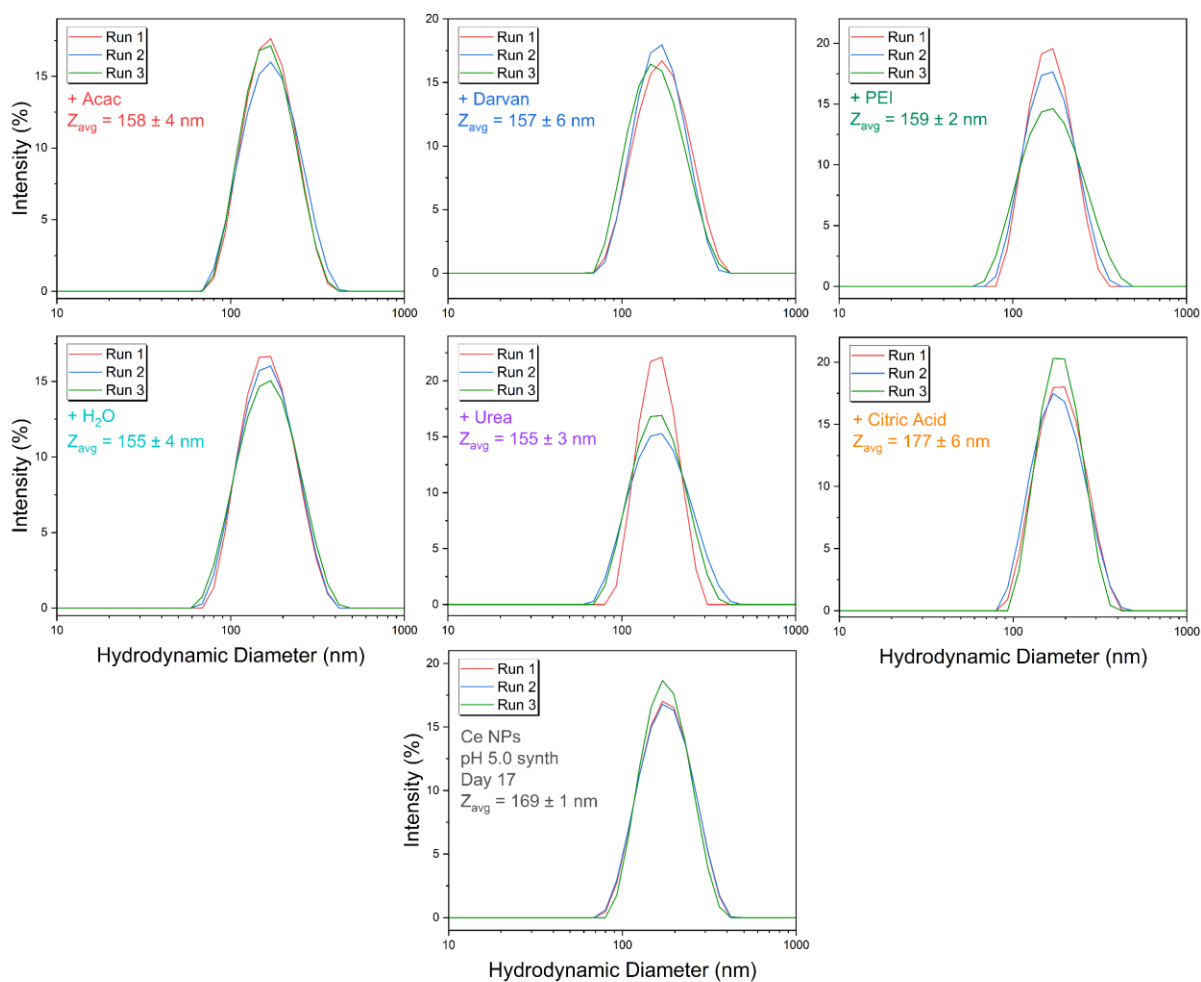


Figure S9. The intensity distribution plots for the indicated additives with a Ce particle batch that was synthesized at pH 5.0.

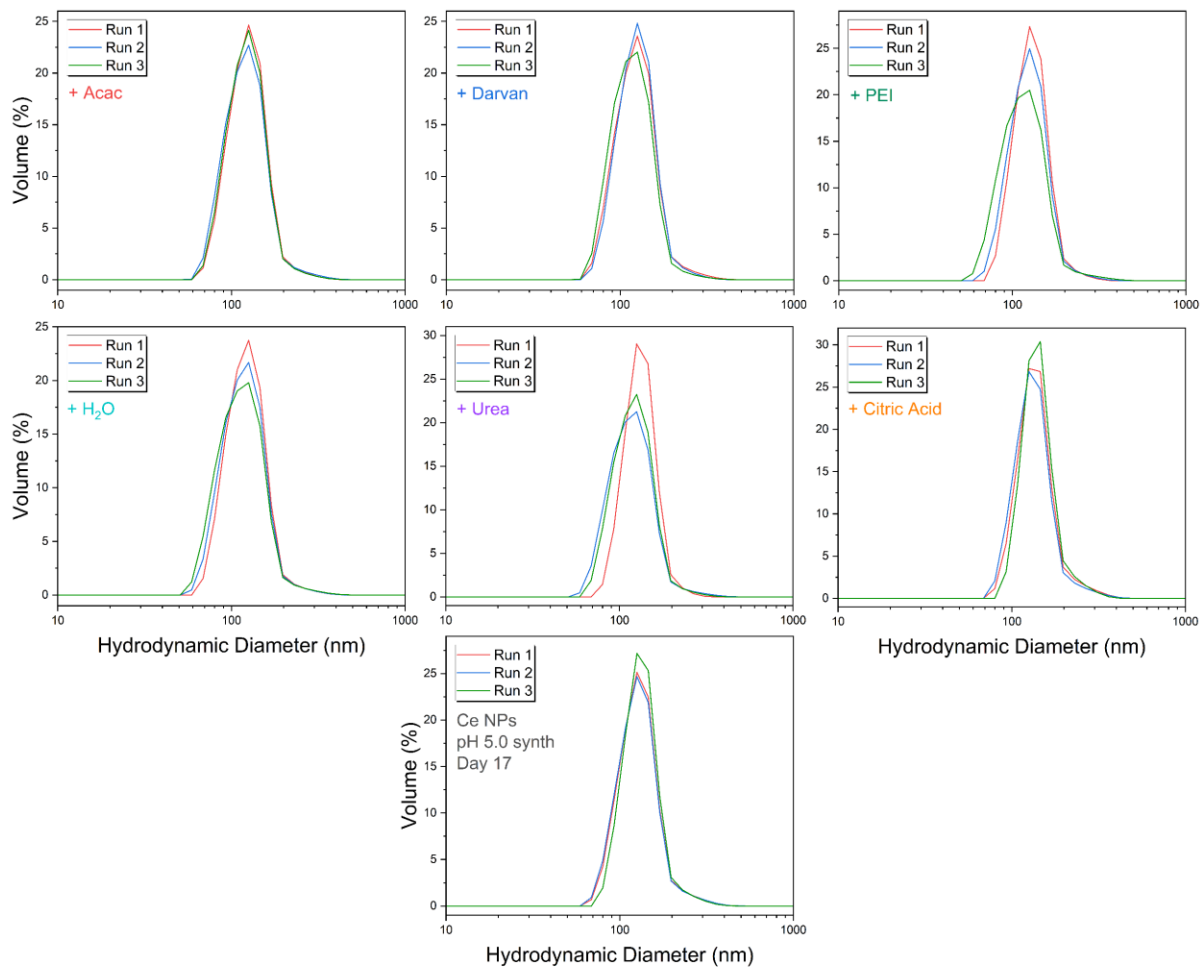


Figure S10. The volume distribution plots for the indicated additives with a Ce particle batch that was synthesized at pH 5.0.

Table S6. DLS and zeta potential results from the Ce particle additive study.

<b>Sample</b>	<b><math>Z_{\text{avg}} \pm 2\sigma</math> (nm)</b>	<b><math>\text{PDI} \pm 2\sigma</math></b>	<b><math>\text{Zeta Potential} \pm 2\sigma</math> (mV)</b>
<b>Control 1</b>	169 ± 1	0.0834 ± 0.0210	+44.1 ± 3.3
<b>+ Acac</b>	158 ± 4	0.0952 ± 0.0038	+42.5 ± 2.4
<b>+ Darvan</b>	157 ± 6	0.110 ± 0.063	-48.2 ± 2.5
<b>+ PEI</b>	159 ± 2	0.121 ± 0.099	+30.6 ± 1.6
<b>+ H<sub>2</sub>O</b>	155 ± 4	0.111 ± 0.013	+45.0 ± 2.4
<b>+ Urea</b>	155 ± 3	0.0758 ± 0.0738	+44.0 ± 1.8
<b>+ Citric Acid</b>	177 ± 6	0.0753 ± 0.0429	+9.19 ± 1.43
<b>Control 2</b>	158 ± 1	0.120 ± 0.005	+54.7 ± 4.3